


Article

Future Evolutions of Precipitation and Temperature Using the Statistical Downscaling Model (SDSM), Case of the Guir and the Ziz Watershed, Morocco

Safae Dafouf *, Abderrahim Lahrach, Hassan Tabyaoui  and Lahcen Benaabidate 

Laboratory of Geo-Resources and Environment, Faculty of Sciences and Techniques, University of Sidi Mohammed Ben Abdellah, Fes 30000, Morocco; abderrahim.lahrach@usmba.ac.ma (A.L.); ;

hassan.tabyaoui@usmba.ac.ma (H.T.); lahcen.benaabidate@usmba.ac.ma (L.B.)

* Correspondence: safaadafouf@gmail.com

Abstract: The current study is essential for obtaining an accurate representation of weather conditions in the Ziz and Guir watersheds, characterized by an arid climate. This study combined climate data from the ERA5 model with data from observation stations in order to evaluate the ERA5 model in Morocco's arid environment and increase the temporal and geographical coverage of climate data. From the data collected, precipitation, minimum and maximum temperatures were predicted under the RCP4.5 and RCP8.5 scenarios by applying the SDSM model in the two watersheds for the 2025 and 2100 periods. These forecasts contribute to the development of adaptation strategies in the face of climate change by giving precise indications of future trends and providing local communities with tools for enhancing their resilience capacity. At all climatic stations, the temperature changes predicted under these scenarios showed a marked positive trend for both minimum and maximum temperatures. By the end of the century, minimum temperatures may increase by 1.84 °C and 2.39 °C under the RCP4.5 and RCP8.5 scenarios, respectively. Similarly, maximum temperatures may increase by 1.78 °C and 2.9 °C under the RCP4.5 and RCP8.5 scenarios, respectively. In addition, the precipitation forecast under the RCP 4.5 scenario showed a significant negative trend at the Ait Haddou station, while under the RCP 8.5 scenario, significant negative trends were predicted for the Sidi Hamza, Ait Haddou, Tit N'Aissa, and Bouanane stations.

Keywords: statistical downscaling model; Southeastern Morocco; future temperatures; future precipitation



Academic Editors: Leszek Sobkowiak, Arthur Mynett and David Post

Received: 18 December 2024

Revised: 12 January 2025

Accepted: 14 January 2025

Published: 24 January 2025

Citation: Dafouf, S.; Lahrach, A.; Tabyaoui, H.; Benaabidate, L. Future Evolutions of Precipitation and Temperature Using the Statistical Downscaling Model (SDSM), Case of the Guir and the Ziz Watershed, Morocco. *Earth* **2025**, *6*, 4. <https://doi.org/10.3390/earth6010004>

Copyright: © 2025 by the authors. Licensee MDPI, Basel, Switzerland. This article is an open access article distributed under the terms and conditions of the Creative Commons Attribution (CC BY) license (<https://creativecommons.org/licenses/by/4.0/>).

1. Introduction

Climate change poses a significant threat to Africa due to the continent's limited adaptive capacity and reliance on climate-sensitive sectors like agriculture [1]. According to the Intergovernmental Panel on Climate Change (IPCC) [2], rising GHG concentrations, particularly carbon dioxide, may cause an increase in global surface temperature of between 1.4 and 5.8 °C by the end of the century. Across Africa, average annual temperatures are projected to rise by 3 to 6 °C by the end of the 21st century under the high-emission scenario RCP8.5. In contrast, precipitation projections are more uncertain, exhibiting significant spatial variability and strong seasonal dependence [3,4]. Specifically, the northern and southern regions of Africa are expected to experience reduced precipitation, while central areas may see increased rainfall [4]. Furthermore, water resources are foreseen to be severely affected, with annual water discharge potentially dropping by 15–45% in a world

that might be 2 °C warmer [5]. This will worsen existing water scarcity problems, with a particular impact on rain-fed agriculture, which accounts for 70% of the agricultural sector [5].

Global climate variables can be simulated using General Circulation Models (GCMs), which take into account the impact of greenhouse gases in the atmosphere and the ensuing global climate change [6]. However, their broad spatial resolution limits their usefulness for assessing regional and local impacts. To overcome this limitation, downscaling techniques have been developed to produce high-resolution climate scenarios from GCM outputs [7]. Downscaled climate projections remain critical for resource management and regional climate.

The Mediterranean region is considered to be a climate change “hotspot”, with temperature projected to increase by 1–5 °C and drought by 10–40% [8]. Situated in the Mediterranean basin, Morocco faces decreasing precipitation and rising temperatures, making it one of the most vulnerable countries to climate change [9].

Future projections consistently indicate substantial warming in Morocco, along with a reduction in annual precipitation across the majority of the country’s regions [10]. These changes are expected to exacerbate drought conditions, particularly in the second half of the century, with moderate droughts likely to predominate and affected areas potentially reaching up to 90% over a six-year period [11].

Furthermore, ref. [12] proposed the adoption of downscaling models to more accurately simulate the climate of central and southern regions in Morocco, which are strongly affected by geographical factors. Refs. [13,14] found a decrease in the wet periods and the intensity of precipitation for the 2030–2050 period, based on simulations obtained from the regional climate model (RCM) piloted by ECHAM5 (scenario A1B). In the same vein, ref. [15] noted a reduction in total precipitation at many stations in Morocco for the years 2021–2050 according to the A1B scenario, by applying a set of various RCMs.

The present study aims to assess future climate parameters in the Ziz and Guir catchments between the years 2025–2100 by combining data from climate stations and the ERA5 model. Forecasting precipitation and minimum and maximum temperatures are of vital importance in this arid region, given the vulnerability of these areas to extreme weather conditions. This makes it a powerful tool for policy-makers, managers, and researchers willing to develop resilience strategies adapted to the specific local contexts of these regions. In this framework, the SDSM model is being used to forecast future climate change conditions under the RCP 4.5 and 8.5 (Representative Concentration Pathway) scenarios.

2. Materials and Methods

2.1. Study Area

The study area belongs to the large Guir, Ziz, Rheris, and Maider watersheds, encompassing two adjacent watersheds in southeastern Morocco: The Guir watershed and the Ziz watershed, located precisely between parallels 5°40' and 2°00' W and meridians 33°00' N and 30°57' N. Covering an area of 26,760.15 km² (Figure 1), this area is limited to the east by the Algerian–Moroccan border, to the north by the Haut Moulouya basin and to the southeast by the Rheris watershed.

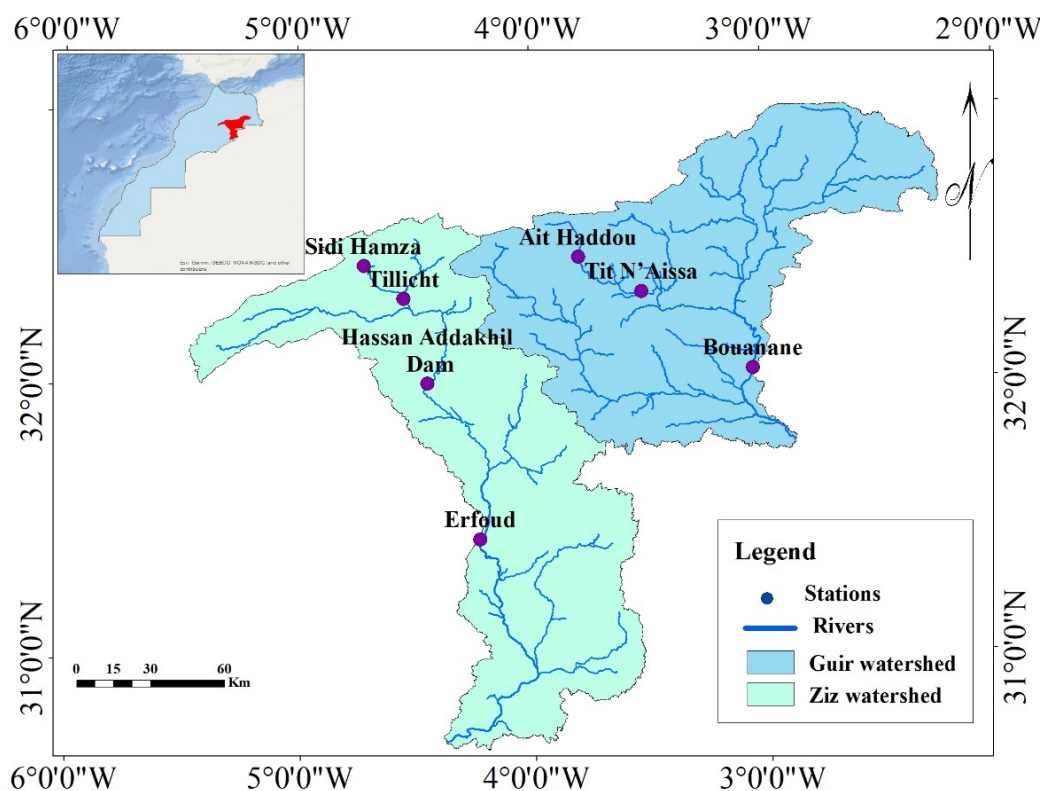


Figure 1. Geographical situation of the study area.

The forecasts of the precipitation and of the minimum and maximum temperature were carried out on various stations of the Ziz and Guir watersheds, distributed at different altitudes, that is the stations Sidi Hamza, Tillicht, Hassan Adakhil dam and Erfoud in the Ziz watershed, and the stations Ait Haddou, Tit N'Aissa and Bouanane in the Guir watershed.

2.2. Data Collection

The data used in this study are daily climatic data, specifically precipitation, and minimum and maximum temperatures, obtained from two sources: the Agency of the Hydraulic Basin of Guir-Ziz-Gheris (ABHGZR) and the ERA5 reanalysis dataset. The ABHGZR provided daily precipitation data for the Sidi Hamza, Tillicht, Hassan Addakhil dam, and Erfoud stations. However, to ensure complete data coverage, particularly for stations with unavailable station data, the ERA5 reanalysis dataset was used to supplement the station observations.

The ERA5 dataset provided daily precipitation data for the Ait Haddou, Tit N'Aissa, and Bouanane stations, as well as minimum and maximum temperature data for all stations. The integration of ERA5 data ensured consistent data coverage across the study area. Indeed, the ERA5 model is widely recognized for its high temporal and spatial resolution, offering significantly improved accuracy compared to earlier global reanalyses [16].

2.3. ERA5 Data

ERA5 is the fifth generation of reanalysis models made available by the Copernicus Climate Change Service (C3S). This service belongs to the six information services proposed by the Copernicus Earth Observation program and produced by the European Centre for Medium-Range Weather Forecasts (ECMWF). The ERA5 presents estimates at a spatial resolution of $0.25^\circ \times 0.25^\circ$ and an hourly temporal resolution, covering the period from 1940 to the present day, for many parameters relating to the atmosphere, ocean waves, and land surface, by combining historical observations with climate model data. This

approach makes it possible to obtain a complete and globally coherent data set through data assimilation.

For this study, hourly data for total precipitation and temperature at 2 m from the ERA5 reanalysis dataset were retrieved for the period 1997–2023 via the CDS interface of C3S (<https://cds.climate.copernicus.eu/#!/home>, accessed on 12 June 2024) using the cdsapiPython package. Using Python, the hourly data were aggregated on a daily scale, and the daily minimum and maximum temperatures were calculated.

The use of ERA5 data in this study was essential to provide climatic data for locations without station observations, ensuring comprehensive data coverage for the application and validation of the SDSM model.

2.4. Methodology

The Statistical Downscaling Model (SDSM), developed by Wilby et al. [17] and used in this study, integrates a weather generator with a multiple linear regression technique. This model is less computationally demanding and easily applicable, making it a practical tool for downscaling climate data. In terms of data requirements, SDSM relies on basic predictor variables from Global Climate Models (GCM) outputs and local observational data, which are typically available for most regions. In contrast, dynamical downscaling methods use regional numerical models that incorporate comprehensive physical processes. Although these methods are grounded in physical principles, they are computationally expensive [18] and therefore require significant computing time [19]. Several studies have compared statistical and dynamical downscaling approaches, showing that they often produce comparable results [18,20,21]. Furthermore, when compared to machine learning models, SDSM has demonstrated greater efficiency and reliability in various applications [22].

The Canadian Earth System Model (CanESM2) from the Coupled Model Intercomparison Project Phase 5 (CMIP5) was utilized in this study to generate climate projections based on Representative Concentration Pathways (RCPs) 2.6, 4.5, and 8.5. CanESM2 has been widely used and proven in the projection of temperature and precipitation trends in various regional climate studies [23–27]. Additionally, it is fully compatible with the Statistical Downscaling Model (SDSM), which requires predictor variables from GCM. Furthermore, CanESM2 predictors are readily available in a format suitable for statistical downscaling. Although CMIP6 represents a more recent generation of climate models, CMIP5 data remain a widely used benchmark in many studies, particularly those employing statistical downscaling methods such as SDSM. The use of CMIP5 scenarios also ensures comparability with prior studies in the region, which frequently rely on these scenarios for projecting climate trends.

RCP scenarios represent different levels of greenhouse gas emissions and their potential impacts on future climate. Earth system models simulate carbon emissions compatible with these scenarios, showing substantial model spread but general consistency with integrated assessment models [28]. For RCP2.6, models project an average 50% emission reduction by 2050 from 1990 levels, with some requiring sustained negative emissions [28]. However, achieving the 2 °C target may be challenging, as simulations suggest slightly higher warming [29]. Uncertainties in land carbon uptake are significant, with some models predicting a shift from sink to source within the 21st century [30]. Key factors affecting allowable emissions include aerosol forcing, climate sensitivity, and carbon cycle parameters [30].

This study focused on analyzing climate projections under the RCP 4.5 and RCP 8.5 scenarios, which exhibited clear trends in the analyzed parameters. The RCP 2.6 scenario was excluded from the analysis, as it showed no significant trends for the two parameters

under study. The predictor variables were derived from CanESM2 results and data from the National Centers for Environmental Prediction (NCEP)/National Center for Atmospheric Research (NCAR) Reanalysis Project 1. These predictor variables were obtained from specific spatial domains corresponding to two grid files in the South-Eastern zone of Morocco. The file BOX_127X_44Y, with a center point at longitude -5.625° and latitude 32.091° N, covers an area approximately between -7.03125° and -4.21875° longitude and 30.68475° and 33.49725° latitude. This grid box was used to extract predictor variables for the Sidi Hamza, Tillicht, Hassan Addakhil Dam, and Erfoud stations. The file BOX_128X_44Y, with a center point at longitude -2.8125° and latitude 32.091° N, covers an area approximately between -4.21875° and -1.40625° longitude and 30.68475° and 33.49725° latitude. This grid box was used for the Ait Haddou, Tit N'Aissa, and Bouanane stations. These files were downloaded from the Canadian Climate Data and Scenarios website (<https://climate-scenarios.canada.ca/>, accessed on 14 June 2024), based on the CanESM2 model with a grid resolution of approximately 2.8125° by 2.8125° .

To ensure the selection of the most relevant predictor variables, a correlation analysis was conducted between the climatic parameters and the predictor variables. This approach identified the variables that were most strongly related to the observed parameters, improving the accuracy of the downscaling process. Following model calibration, projections of climate parameters were generated for the period 2025–2100, based on the RCP 4.5 and RCP 8.5 scenarios. Figure 2 illustrates the sequence of steps involved in the SDSM model process, from predictor selection to the generation of future climate projections.

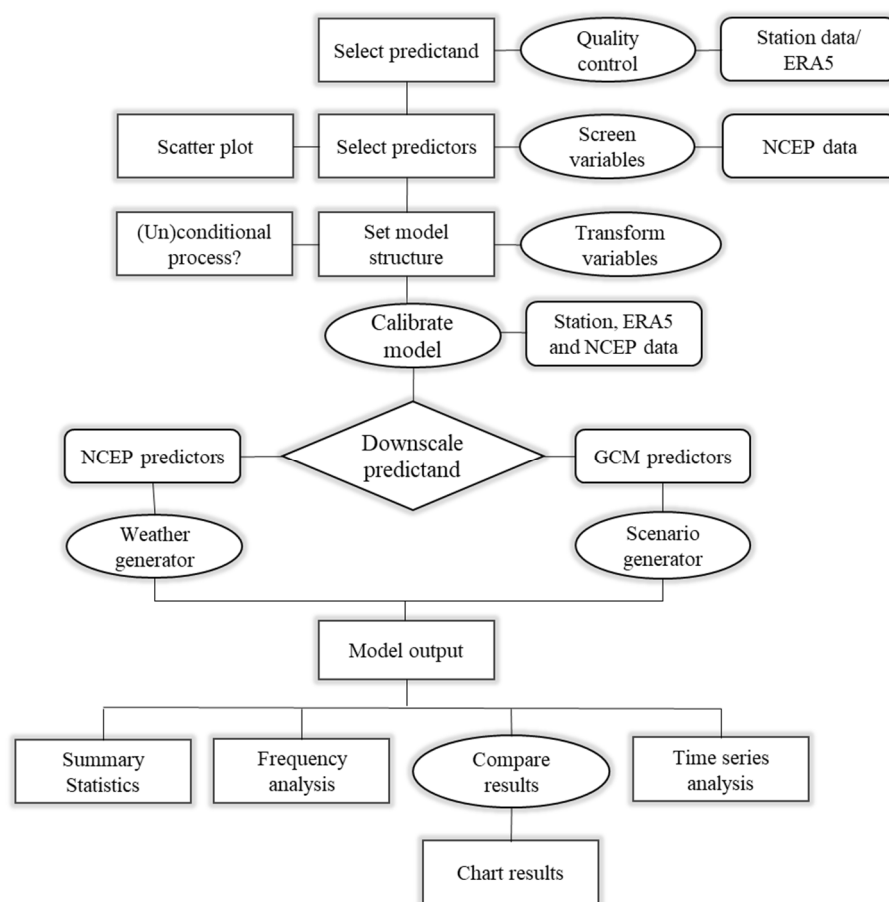


Figure 2. SDSM 4.2 process [17].

A trend analysis was conducted using two non-parametric tests on the predicted climate parameter time series: the Mann–Kendall test [31,32], and the Sen’s slope test [33].

The Mann–Kendall test is a nonparametric method used to determine the presence of a statistically significant trend in a time series. In this test, the null hypothesis (H0), which assumes no trend, is accepted if the *p*-value exceeds the chosen alpha significance level. The direction of the trend is determined by the Mann–Kendall statistical coefficient (Z value), as shown in Equation (1). A positive Z value ($Z > 0$) indicates an upward trend, while a negative Z-value ($Z < 0$) indicates a downward trend.

$$Z = \begin{cases} \frac{S-1}{\sqrt{Var(S)}} & S > 0 \\ 0 & S = 0 \\ \frac{S+1}{\sqrt{Var(S)}} & S < 0 \end{cases} \quad (1)$$

where *S* is the test statistic calculated using Equation (2), with X_i and X_j representing the time series data at time points *i* and *j*, respectively. The sign function $sgn(X_j - X_i)$ returns +1 if $X_j > X_i$, 0 if $X_j = X_i$, and −1 if $X_j < X_i$.

$$S = \sum_{i=1}^{n-1} \sum_{j=i+1}^n sgn(X_j - X_i) \quad (2)$$

The variance of *S*, denoted as $Var(S)$, is calculated to account for ties (equal values) in the data. The formula for $Var(S)$ is given by Equation (3):

$$Var(S) = \frac{n(n-1)(2n+5) - \sum_{t=1}^m t_t(t_t-1)(2t_t+5)}{18} \quad (3)$$

where *n* is the total number of observations in the time series, *m* is the number of tied groups (groups of equal values), and t_t is the number of data points in the *t*th tied group.

The Sen’s slope [33] was used to estimate the magnitude of the trend. It is a non-parametric method that calculates the slope as the median of all possible pairwise slopes between data points in a time series. The slope between two data points X_j and X_k (where $j > k$) is calculated as:

$$S_i = \frac{X_j - X_k}{j - k} \quad (i = 1, \dots, N) \quad (4)$$

where *N* is the total number of slope values calculated from all possible pairs of data points, and *i* represents each slope calculated from *N* pairs of data points.

The Sen’s slope is then obtained by calculating the median of these *N* slope values:

$$Q_{med} = \begin{cases} S_{\frac{N+1}{2}}, & \text{if } N \text{ is odd} \\ \frac{S_{\frac{N}{2}} + S_{\frac{N+2}{2}}}{2}, & \text{if } N \text{ is even} \end{cases} \quad (5)$$

2.5. Statistical Analysis

The ERA5 Reanalysis Model data were evaluated for their performance using widely applied statistical indices, calculated in R with the stats and Metrics packages. These statistical indices primarily include the coefficient of determination (R^2) [34], which quantifies the proportion of the total variance in the observed data explained by the ERA5 model data. Additionally, the mean error (ME), mean absolute error (MAE), and root mean square error (RMSE) were used to evaluate the accuracy of the ERA5 data compared to observed values. ME measures the average deviation between observed and modeled values, MAE reflects the magnitude of the mean error regardless of direction, and RMSE emphasizes larger errors by calculating the square root of the average squared differences between observed and modeled values.

3. Results

3.1. Comparison of Climate Data from the ERA5 Reanalysis Model and Observed Station Climate Data

The precipitation data from the ERA5 reanalysis model applied in this study are compared with those observed at the climate stations in the Guir watershed, which are Ait Haddou, Tit N'Aissa, and Bouanane. In addition, the temperature data from the ERA5 model are compared with those from the Hassan Adakhlil dam, Erfoud, and Bouanane stations, which are the only stations with temperature data. This comparison is carried out on a monthly scale by calculating statistical indices (R^2 , ME, MAE, and RMSE). The results showed good adequacy between the two data sources (Table 1), particularly for the temperature data, where R^2 ranged from 0.85 to 0.97 and from 0.60 to 0.70 for the precipitation data. Furthermore, the RMSE values range from 1.34 to 4.25, and the MAE values are below 5.04. This indicates a high degree of consistency between the climate data from the ERA5 model and those observed by the stations.

Table 1. Statistical indices of data used.

Station	Station	R^2	ME	MAE	RMSE
Hassan Addakhlil dam	T min	0.851	−2.58	3.27	3.84
	T max	0.934	−1.8	2.22	2.67
Erfoud	T min	0.954	0.97	1.43	2.02
	T max	0.974	−0.43	0.9	1.34
Bouanane	T min	0.920	0.02	1.57	2.24
	T max	0.975	−0.60	0.91	1.40
	Precipitation	0.705	−0.55	4.98	3.01
Ait Haddou	Precipitation	0.604	0.60	5.04	3.78
Tit N'Aissa	Precipitation	0.643	−0.20	4.86	4.25

3.2. Selection of Predictor Variables

The selection of predictor variables provided by NCEP/NCAR was essential for developing a model to predict various climatic factors. A correlation analysis was conducted to identify the predictor variables most strongly associated with the target climate variables. Two statistical parameters guided the selection process: the correlation coefficient (r) and the p -value. All selected predictor variables demonstrated statistically significant correlations, with p -values less than 0.0001. To further validate the relationships, scatter plots were used to confirm and verify the associations between the predictor variables and the climatic factors. Based on this analysis, the set of predictor variables was selected for the creation of the calibrated model.

The predictors selected for maximum and minimum temperature at all studied stations are the mean temperature at 2 m and the vorticity at 500 hPa (Table 2), which measures air rotation at this altitude in the atmosphere. For precipitation, the predictor variables vary spatially across the study area (Table 3), reflecting the complexity of the meteorological processes responsible for precipitation.

Table 2. Selection of predictive variables for temperatures.

	Station	Predictive Variables	Predictor Description	r
Minimum temperature	Sidi Hamza			0.634 0.721
	Tillicht	p5_z	500 hPa vorticity	0.692 0.735
	Hassan Addakhil dam			0.625 0.766
	Erfoud			0.651 0.712
	Ait Haddou	temp	Surface mean temperature	0.670 0.720
	Tit N'Aissa			0.632 0.754
	Bouanane			0.676 0.783
	Maximum temperature	Sidi Hamza		
Tillicht		p5_z	500 hPa vorticity	0.682 0.753
Hassan Addakhil dam				0.671 0.746
Erfoud				0.626 0.750
Ait Haddou		temp	Surface mean temperature	0.644 0.762
Tit N'Aissa				0.605 0.775
Bouanane				0.653 0.780

Table 3. Selection of predictive variables for precipitation.

Climatic Parameter	Stations	Predictive Variables	Predictor Description	r
Precipitation	Sidi Hamza	p8_zh,	850 hPa divergence	0.682
		temp	Surface mean temperature	0.730
	Tillicht	prcp,	Surface precipitation	0.691
		p5_zh	500 hPa divergence	0.576
	Hassan Addakhil dam	p1_f,	Surface air flow strength	0.714
p500		500 hPa geopotential height	0.682	
Erfoud	p1_z,	Surface vorticity	0.625	
	p1_zh,	Surface divergence	0.590	

Table 3. *Cont.*

Climatic Parameter	Stations	Predictive Variables	Predictor Description	r
Precipitation	Ait Haddou	mslp,	Mean sea level pressure	0.583
		p1_v,	Surface meridional velocity	0.645
		p500	500 hPa geopotential height	0.670
	Tit N’Aissa	mslp,	Mean sea level pressure	0.574
		p850	850 hPa geopotential height	0.667
		Bouanane	p1_v,	Surface meridional velocity
p500	500 hPa geopotential height		0.680	

3.3. Calibration and Validation of the SDSM Model

The calibration (period 1997–2015) and the validation (period 2016–2023) of the SDSM model are conducted by the calculation of statistical indices, notably the coefficient of determination (R^2) and the root mean square error (RSME), to assess the model’s performance at the studied climate stations. Table 4 presents the results of the calculation, highlighting the model’s performance in simulating and supplying rainfall data as well as maximum and minimum temperatures. For all climate stations, the coefficient of determination (R^2) values for the climate parameters studied range from 0.66 to 0.77. The root mean square error (RSME) values range from 1.52 to 3.84.

Table 4. Calculation of statistical indices for the calibration (1997–2015) and validation (2016–2023) of the SDSM model at the climate stations studied.

Stations	Climatic Parameters	RMSE		R^2	
		(1997–2015)	(2016–2023)	(1997–2015)	(2016–2023)
Sidi Hamza	Precipitation	3.41	3.02	0.70	0.75
	T max	2.87	2.43	0.72	0.76
	T min	3.51	3.12	0.68	0.72
Tillicht	Precipitation	3.23	2.86	0.69	0.71
	T max	3.37	3.05	0.70	0.74
	T min	3.44	3.08	0.68	0.72
Hassan Adakhil dam	Precipitation	3.84	3.25	0.66	0.70
	T max	3.21	2.89	0.70	0.76
	T min	3.54	3.16	0.68	0.73
Erfoud	Precipitation	3.68	3.23	0.67	0.70
	T max	3.14	2.78	0.68	0.72
	T min	3.34	2.97	0.66	0.71
Ait Haddou	Precipitation	2.81	2.55	0.71	0.76
	T max	3.17	1.52	0.75	0.77
	T min	2.46	1.62	0.73	0.75
Tit N’Aissa	Precipitation	3.04	2.83	0.67	0.70
	T max	2.27	1.84	0.69	0.72
	T min	2.98	2.52	0.72	0.75
Bouanane	Precipitation	3.43	2.94	0.68	0.74
	T max	2.23	1.65	0.70	0.73
	T min	3.56	1.88	0.69	0.75

3.4. Comparison of Observed and Simulated Data

The comparison of observed and simulated data shows that the simulated precipitation data are similar or very close to the observed data (Figure 3), suggesting that the SDSM model has a good ability to downscale precipitation. Additionally, the simulated minimum and maximum temperature data show a nearly perfect match with the observed data across all months and stations. Given this near-perfect match, we have focused solely on presenting the precipitation data (Figure 3). These results highlight the relevance of the selected predictive variables for both precipitation and temperature modeling at the studied stations.

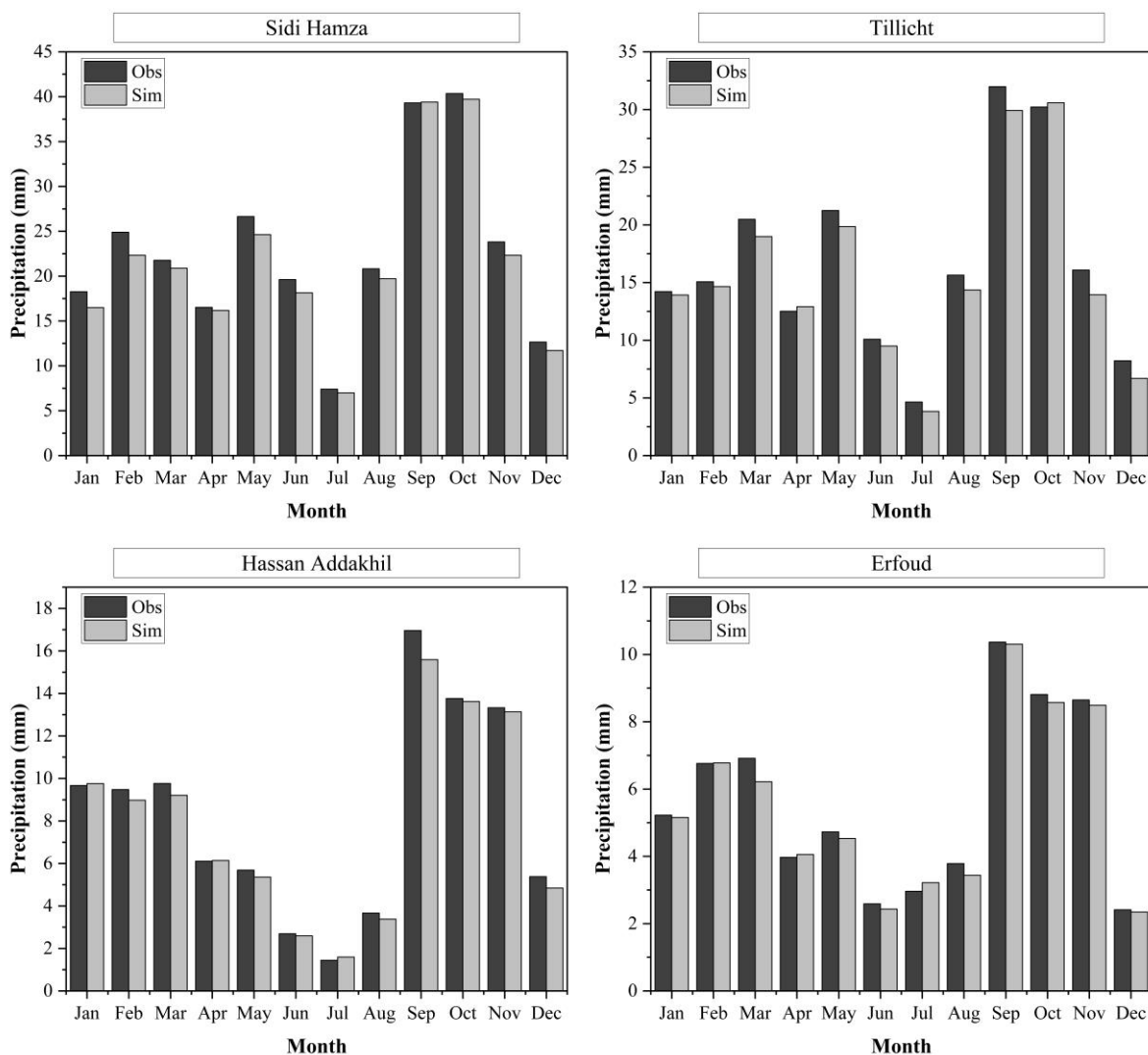


Figure 3. Cont.

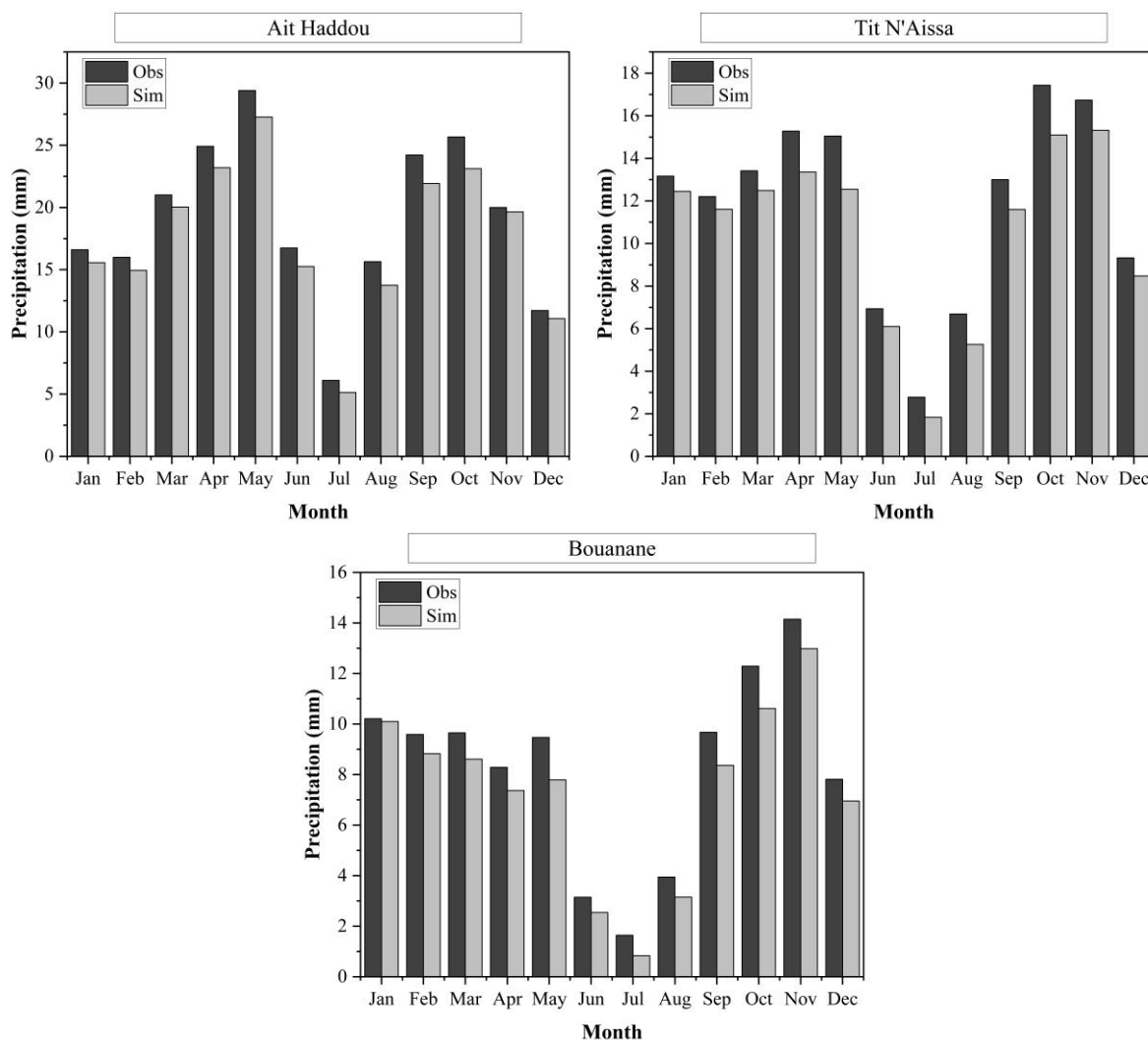


Figure 3. Validation of SDSM performance for precipitation by comparing the observed and the simulated precipitation for the period 1997–2023.

3.5. Analysis of Historical and Predicted Climate Parameters Trends

To investigate the potential influence of the downscaling procedure on the climate change signal, we analyzed trends in historical and downscaled data, as well as Weather Generator series produced by SDSM based on the NCEP-NCAR reanalysis data.

The analysis of historical precipitation (1997–2023) revealed non-significant trends ($p > 0.05$) across all stations (Table 5). This result suggests that precipitation variability during the historical period does not exhibit a consistent or significant directional change. For the future precipitation projections (2025–2100), the results revealed a significant negative trend at the 5% significance threshold under the RCP 4.5 scenario, at the Ait Haddou station (Table 6). Under the RCP 8.5 scenario, there was a significant negative trend at the Sidi Hamza, Ait Haddou, Tit N’Aissa, and Bouanane stations, and a significant positive trend at the Hassan Addakhil dam station. These results suggest that future precipitation trends reflect the climate change signal estimated by the model, especially under the RCP8.5 scenario. The difference between historical and future trends highlights the increasing prominence of climate change impacts on precipitation patterns in the latter half of the 21st century.

Table 5. Mann-Kendall (Z and *p* value) and Sen slope tests for historical precipitation and minimum and maximum temperatures at stations of the Ziz and Guir watersheds.

Stations	Climatic Parameters	MK Z Value	MK <i>p</i> Value	Sen's Slope	Trend
Sidi Hamza	Precipitation	−0.125	0.900	−0.146	NS *
	T min	0.801	0.423	0.003	NS
	T max	0.018	0.036	0.114	S **
Tillicht	Precipitation	0.667	0.505	0.961	NS
	T min	0.674	0.500	0.003	NS
	T max	0.049	0.046	0.104	S
Hassan Addakhi dam	Precipitation	−0.188	0.851	−0.325	NS
	T min	0.593	0.553	0.002	NS
	T max	1.104	0.269	0.004	NS
Erfoud	Precipitation	1.751	0.080	1.428	NS
	T min	0.676	0.499	0.003	NS
	T max	0.029	0.039	0.235	S
Ait Haddou	Precipitation	−0.500	0.617	−0.863	NS
	T min	0.661	0.508	0.002	NS
	T max	0.872	0.383	0.003	NS
Tit N'Aissa	Precipitation	−0.208	0.835	−0.177	NS
	T min	0.720	0.471	0.003	NS
	T max	0.871	0.383	0.003	NS
Bouanane	Precipitation	−0.167	0.867	−0.214	NS
	T min	0.485	0.627	0.002	NS
	T max	0.047	0.031	0.144	S

* not significant at 5% significance level ($p > 0.05$). ** significant at 5% significance level ($p < 0.05$).

The analysis of historical temperature trends (1997–2023) revealed distinct patterns for minimum and maximum temperatures. No significant trends were detected for minimum temperatures at any station ($p > 0.05$). In contrast, significant positive trends were observed for maximum temperatures at stations Sidi Hamza, Tillicht, Erfoud, and Bouanane (Table 5). For the forecasted period (2025–2100), significant positive trends were observed for minimum and maximum temperatures at all climatic stations under the RCP 4.5 and RCP 8.5 scenarios ($p < 0.05$, Table 6). These results indicate an intensification of warming trends in the future, in line with anticipated impacts of climate change predicted by the scenarios. The contrast between historical and predicted trends highlights the evolving influence of climate change on regional temperature dynamics, with a clear amplification of warming trends in the future.

The analysis of the Weather Generator series revealed no significant trends ($p > 0.05$) in the climatic variables across all stations for the historical period (Table 7). This result indicates that the predictor variables used in the downscaling process do not exhibit inherent trends that could influence the projected series. Consequently, the trends observed in the downscaled series are primarily attributable to the GCM projections rather than the predictors. The comparison between the Weather Generator series and the downscaled series indicates that the climate change signal observed in the projections is primarily driven by the GCM outputs.

Table 6. Mann–Kendall (Z and *p* value) and Sen slope tests for predicted precipitation and minimum and maximum temperatures at stations of the Ziz and Guir watersheds.

Stations	Climatic Parameters	MK Z Value		MK <i>p</i> Value		Sen’s Slope		Trend	
		RCP4.5	RCP8.5	RCP4.5	RCP8.5	RCP4.5	RCP8.5	RCP4.5	RCP8.5
Sidi Hamza	Precipitation	−0.152	−0.4389	0.053	2.12×10^{-8}	−0.136	−0.559	NS *	S **
	T min	0.0078	0.0231	0.0424	0.0296	0.158	0.185	S	S
	T max	0.014	0.0401	0.0326	0.007	0.233	0.259	S	S
Tillicht	Precipitation	0.0449	−0.148	0.569	0.059	0.039	−0.143	NS	NS
	T min	0.0028	0.0292	0.0408	0.0186	0.254	0.266	S	S
	T max	0.0148	0.0332	0.039	0.0134	0.244	0.287	S	S
Hassan Addakhi dam	Precipitation	−0.0632	0.190	0.422	0.015	−0.052	0.120	NS	S
	T min	0.0068	0.0269	0.0360	0.0223	0.173	0.189	S	S
	T max	0.0131	0.0283	0.0383	0.0200	0.183	0.196	S	S
Erfoud	Precipitation	0.0968	−0.05.68	0.218	0.470	0.034	−0.020	NS	NS
	T min	0.0073	0.0242	0.042	0.0473	0.143	0.156	S	S
	T max	0.0066	0.0329	0.046	0.0437	0.126	0.148	S	S
Ait Haddou	Precipitation	−0.28	−0.673	0.0003	$<2.2 \times 10^{-16}$	−0.193	−0.770	S	S
	T min	0.0094	0.0234	0.038	0.0249	0.235	0.265	S	S
	T max	0.0138	0.0484	0.031	0.029	0.256	0.281	S	S
Tit N’Aissa	Precipitation	−0.072	−0.408	0.358	1.92×10^{-7}	−0.173	−0.195	NS	S
	T min	0.0128	0.0268	0.044	0.0326	0.176	0.185	S	S
	T max	0.0079	0.0447	0.031	0.043	0.123	0.151	S	S
Bouanane	Precipitation	0.0014	−0.408	0.989	1.92×10^{-7}	0.001	−0.189	NS	S
	T min	0.0081	0.0265	0.039	0.0331	0.147	0.160	S	S
	T max	0.0088	0.0457	0.032	0.039	0.160	0.172	S	S

*: not significant at 5% significance level ($p > 0.05$). **: significant at 5% significance level ($p < 0.05$).

Table 7. Mann–Kendall (Z and *p*-value) and Sen slope tests for Weather Generator series at Ziz and Guir watershed stations.

Stations	Climatic Parameters	MK Z Value	MK <i>p</i> Value	Sen’s Slope	Trend
Sidi Hamza	Precipitation	−0.583	0.560	−0.215	NS
	T min	0.237	0.156	0.070	NS
	T max	0.178	0.092	0.582	NS
Tillicht	Precipitation	0.4176	0.156	0.064	NS
	T min	0.294	0.195	0.016	NS
	T max	0.044	0.201	0.104	NS
Hassan Addakhi dam	Precipitation	−0.375	0.2075	−0.353	NS
	T min	0.034	0.1281	0.134	NS
	T max	0.203	0.140	0.117	NS
Erfoud	Precipitation	0.667	0.0954	0.177	NS
	T min	1.818	0.068	0.161	NS
	T max	0.1957	0.162	0.114	NS
Ait Haddou	Precipitation	0.709	0.478	0.380	NS
	T min	0.322	0.107	0.128	NS
	T max	0.938	0.052	0.014	NS
Tit N’Aissa	Precipitation	−0.163	0.567	−0.133	NS
	T min	0.201	0.097	0.059	NS
	T max	0.0871	0.183	0.003	NS
Bouanane	Precipitation	0.583	0.059	0.477	NS
	T min	0.398	0.158	0.090	NS
	T max	0.188	0.102	0.046	NS

3.6. Precipitation Forecasts

The results of precipitation forecasts for the period 2025–2100 according to the RCP4.5 and RCP8.5 scenarios are shown in Figure 4.

The precipitation forecast under the RCP4.5 scenario for the Sidi Hamza station showed fluctuations over the period studied. Nevertheless, under the RCP8.5 scenario, the precipitation appears to have a negative trend, with values reaching 191.94 mm in 2089 and 269.13 mm in 2025.

The forecast precipitation results for the Tillicht station also reveal clearly apparent fluctuations and interannual variability under the RCP4.5 scenario. The future rainfall series under the RCP8.5 scenario shows positive peaks in 2034, 2068, and 2074, indicating periods of high precipitation.

For the Hassan Addakhil Dam station, the precipitation values forecast for the period 2025–2100, according to the RCP4.5 and RCP8.5 scenarios, are lower than those forecast for the previous stations owing to its geographical location. These values do not exceed 144.32 mm and 132.40 mm, respectively, under the RCP4.5 and RCP8.5 scenarios.

The annual precipitation will continue to increase towards the South of the Ziz watershed, where the Erfoud station is located. Indeed, the range of precipitation forecast under the RCP4.5 and RCP8.5 scenarios is 50.43 mm to 76.53 mm and 50.40 mm to 78.72 mm, respectively.

In the Guir watershed, the forecast precipitation at the Ait Haddou station shows a downward trend for the RCP4.5 scenario, this trend is particularly evident in the case of the pessimistic RCP8.5 scenario.

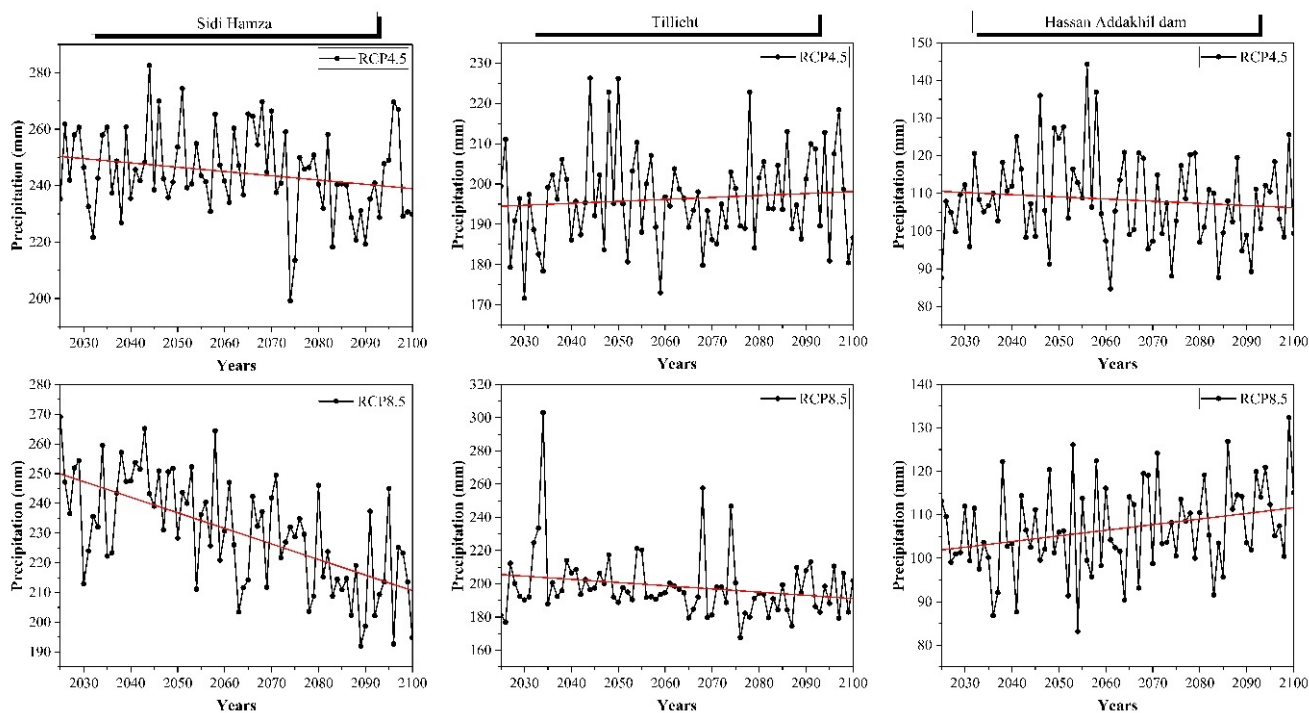


Figure 4. Cont.

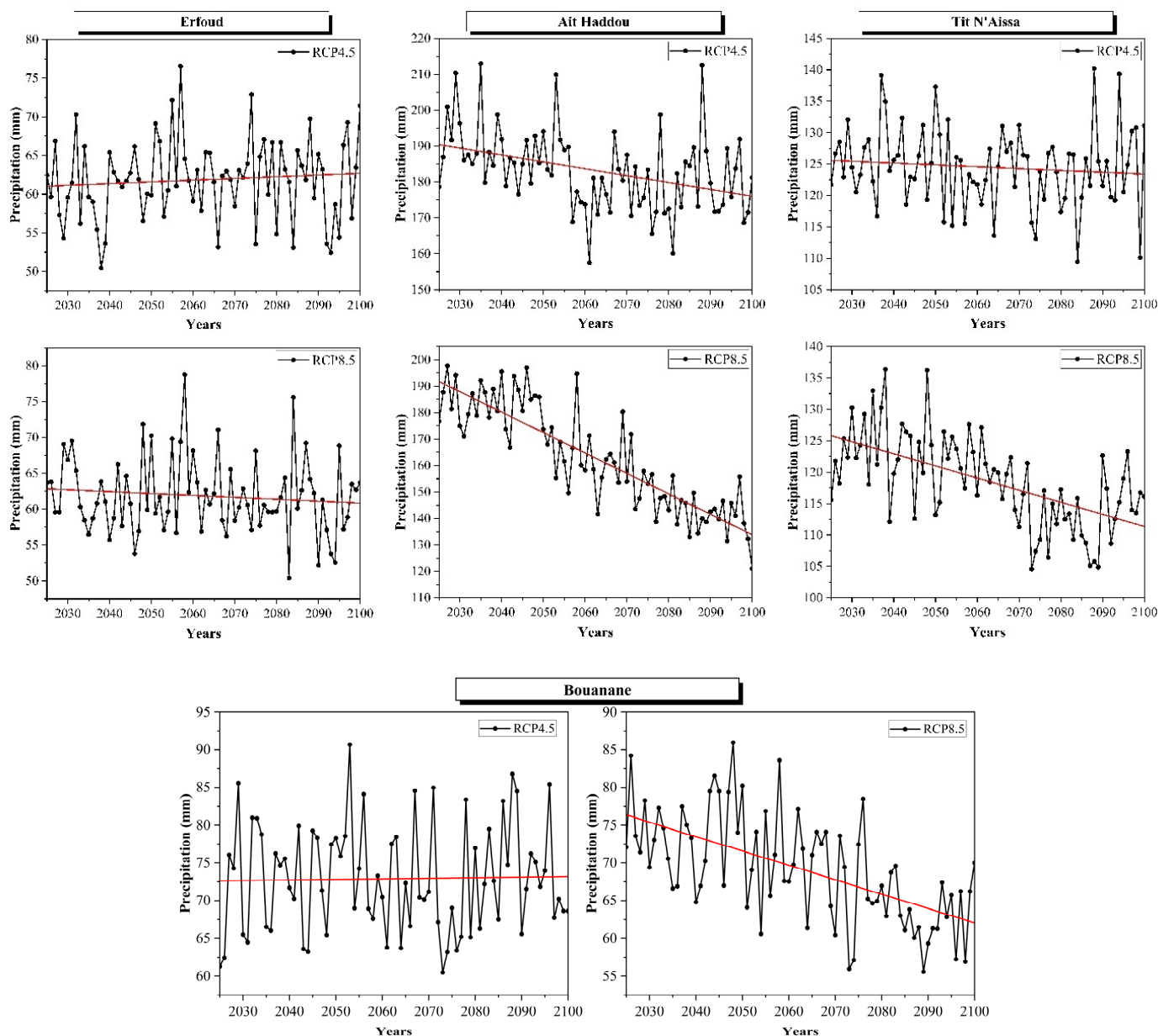


Figure 4. Precipitation evolution of the Ziz and Guir watershed stations for the 2025–2100 period.

At the Tit N’Aissa station, the analysis of the annual precipitation forecast under the RCP4.5 scenario shows interannual variations, with two negative peaks of 109.43 mm and 110.10 mm that will be recorded in 2084 and 2099, respectively. The temporal evolution of precipitation forecast under the RCP8.5 scenario shows a decrease from 2048 onwards.

The downstream of the Guir watershed sits the Bouanane station, which presents the lowest forecast precipitation compared with the other stations in this watershed. The analysis of the annual forecast precipitation for the period 2025–2100 showed fluctuations throughout the time series according to the RCP4.5 scenario. However, the precipitation forecast under the RCP8.5 scenario revealed a downward trend.

3.7. Minimum and Maximum Temperature Forecasts

The forecast of the minimum and maximum temperatures for the periods 2025 and 2100 according to the RCP4.5 and RCP8.5 scenarios is shown in Figure 5.

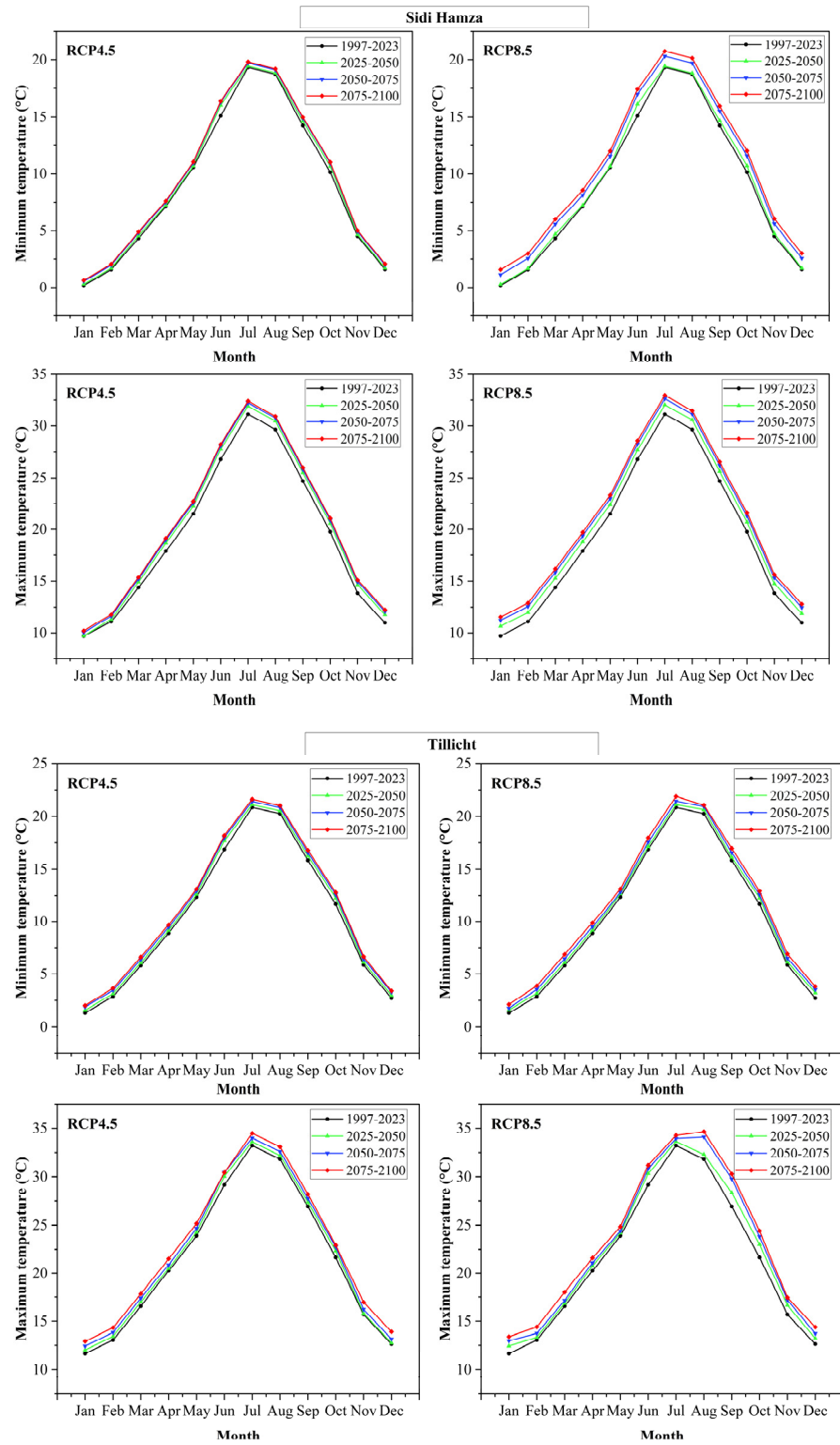


Figure 5. Cont.

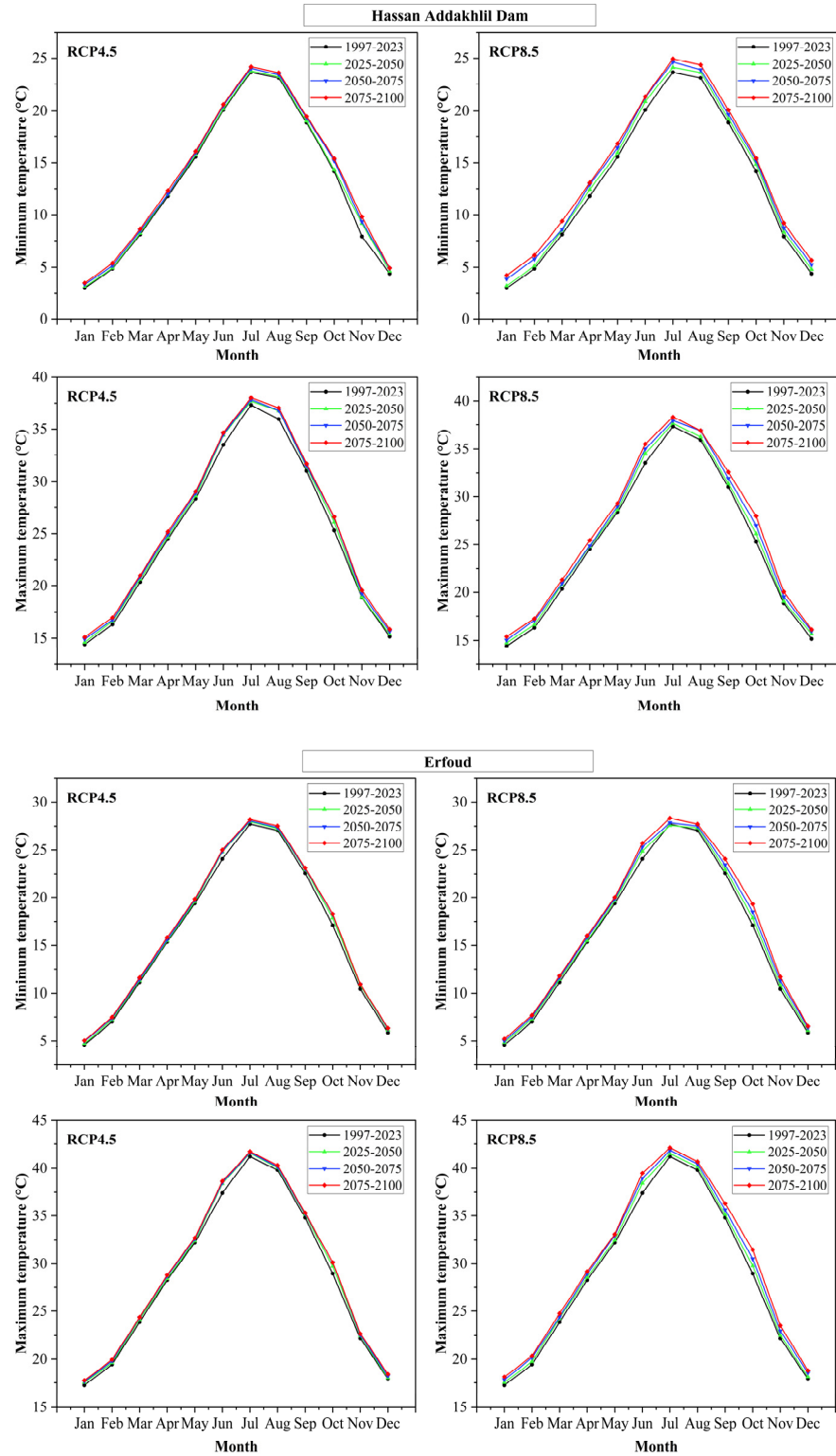


Figure 5. Cont.

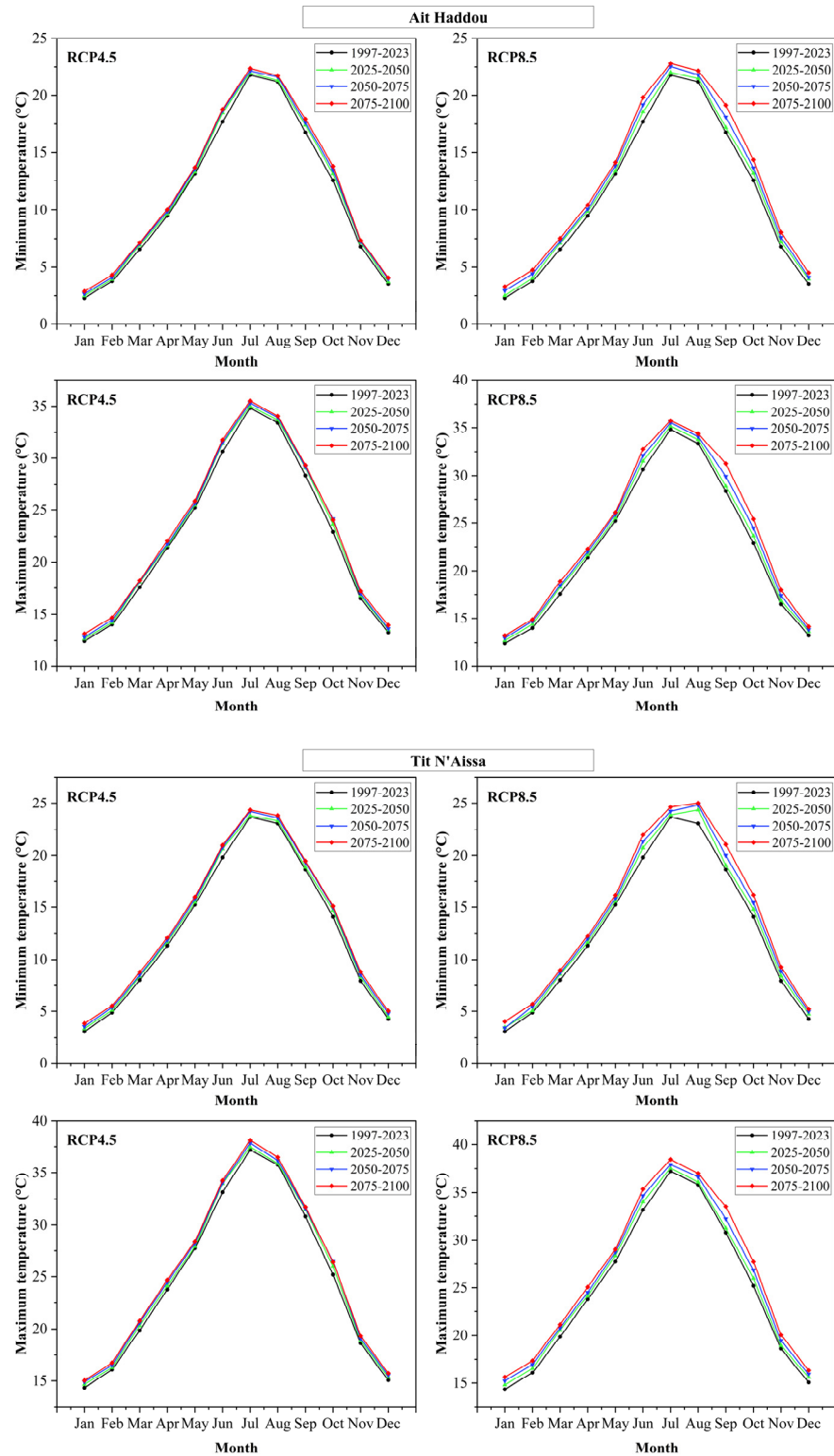


Figure 5. Cont.

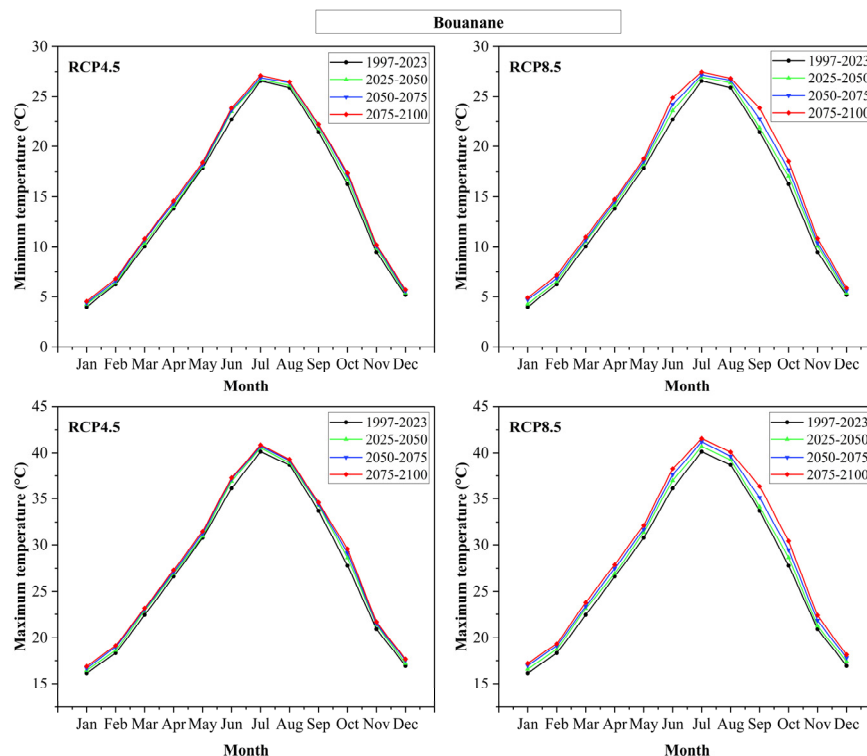


Figure 5. Evolution of predicted minimum and maximum temperatures for the period 2025–2100 in the Ziz and Guir watersheds.

At the Sidi Hamza station, the minimum temperature will rise over the period 2025–2100, this increase being from 0.47 °C to 1.28 °C during the last quarter of the century (2075–2100) according to the RCP4.5 scenario, and 1.39 to 2.30 according to the RCP8.5 scenario. Similarly, the maximum temperature will rise from 0.40 to 1.36 and 2.35, respectively, according to the RCP4.5 and RCP8.5 scenarios.

For the station of Tillicht, it is forecast that the minimum temperatures will increase by 0.68 °C to 1.31 and by 0.76 to 1.23 °C during the period 2075–2100, respectively, according to the scenarios RCP4.5 and RCP8.5. The maximum temperature will also rise by 1.27 °C and 2.52 °C, respectively, under the RCP4.5 and RCP8.5 scenarios, at the end of the century.

As for the Hassan Addakhil dam station, the minimum and maximum temperatures will show an upward trend under both scenarios. Indeed, the minimum temperature values will increase by 0.52 °C to 1.22 °C and by up to 1.84 °C, respectively, according to the RCP4.5 and RCP8.5 scenarios. For the maximum temperature, the increase will be 0.68 °C to 1.26 °C and 0.96 °C to 2.63 °C according to the RCP4.5 and RCP8.5 scenarios, respectively.

The Erfoud station, which is characterized by an arid climate, will experience an increase in the minimum and maximum temperatures, as will the other stations. By the end of the century, the minimum temperature will have risen by 0.47 °C to 1.15 °C and by 0.66 °C to 2.18 °C, respectively, according to the RCP4.5 and RCP8.5 scenarios. For the same scenarios, the maximum temperature will rise by 0.51 °C to 1.21 °C and 0.82 °C to 2.52 °C, respectively.

In the Guir watershed, there is a rising trend in forecast temperatures for both scenarios at the Ait Haddou station. This trend is more marked under the RCP8.5 scenario than the RCP4.5 scenario. Over the period 2075–2100, the minimum temperature will rise under the RCP4.5 and RCP8.5 scenarios by 0.57 °C to 1.21 °C and by 0.99 °C to 2.39 °C, respectively, and the maximum temperature by 0.67 °C to 1.13 °C and by 0.78 °C to 2.9 °C, respectively.

For the Tit N'Aissa station, the temperatures will also record a significant increase. Under the RCP4.5 scenario, the minimum and the maximum temperatures will rise by 0.66 °C to 1.17 °C and 0.68 °C to 1.24 °C, respectively, over the period 2075–2100. Furthermore, according to the RCP8.5 scenario, the minimum and the maximum temperatures will increase by 0.83 °C to 2.39 °C and by 1.17 °C to 2.70 °C, respectively.

The Bouanane station, for its part, will experience an upward trend in temperatures under both scenarios. The minimum temperature will rise by 0.56 °C to 1.16 °C under the RCP4.5 scenario and by 0.73 °C to 2.35 °C under the RCP8.5 scenario. The maximum temperature will also rise by 0.6 °C to 1.78 °C and by 1.02 °C to 2.63 °C, according to the RCP4.5 and RCP8.5 scenarios, respectively.

It is important to emphasize that the maximum increase in the forecast temperatures is recorded in particular during the months of June, September, October, and November. This increase could reflect significant changes in the climate regime, leading to local repercussions, but could also be more widespread. The noticeable rise in temperatures during the month of June suggests that summer will get off to an early start with more intense heat waves. This increase also indicates that the summer season will get increasingly hotter. Further, the significant increase in the months of September, October, and November indicates a prolongation of the annual warm period beyond the summer months.

In addition, the predicted spike in the minimum and the maximum temperatures is much more pronounced under the RCP8.5 scenario than under the RCP4.5 scenario. The latter is a stabilization scenario, which foresees the attenuation of greenhouse gas emissions through ambitious but achievable reduction measures. In contrast, the RCP8.5 scenario is often regarded as a pessimistic scenario of high emissions.

4. Discussion

In the present study, ERA5 climate data were used to complement station data in order to provide an overall climatic forecast for the Ziz and Guir watershed. The results of comparing ERA5 climate data with observed station climate data showed a good fit between the two data sources. These results indicate that ERA5 reanalysis data can be a valuable alternative to station observations in the Guir and Ziz watersheds, which are characterized by an arid climate. The authors of [35,36] showed that ERA5 generally outperforms other reanalysis products in reproducing temperature and precipitation patterns, displaying higher correlations and lower errors compared with station observations. However, reanalysis performance can vary according to location, with better results generally observed in mid-latitude continental regions than in coastal and arctic regions [36].

The SDSM is a widely used tool for generating high-resolution climate change scenarios [37]. SDSM has shown good performance in simulating temperature and precipitation, and good concordance between observed and simulated data, making it a valuable tool for local-scale climate projections [38]. Ref. [39] also revealed satisfactory results in simulating temperature and precipitation in the city of Xingtai, China.

SDSM projections showed a significant downward trend in precipitation under the RCP 4.5 scenario, at the Ait Haddou station. Under the RCP 8.5 scenario, the majority of stations in the study area presented a significant negative trend. Furthermore, in Khyber Pakhtunkhwa, Pakistan, SDSM model projections showed an increase in precipitation in monsoon-dominated areas under the RCP4.5 scenario, while RCP8.5 indicated a decrease [40]. A Moroccan study in the Boufakrane watershed revealed no rainfall trend under the RCP4.5 and RCP8.5 scenarios, but a downward trend under the RCP2.6 scenario [41]. Another Moroccan study for the Souss-Massa and Ouergha watersheds predicted a decrease in precipitation for the RCP4.5 and RCP8.5 scenarios [42]. In the Subansiri river

basin in Northeast India, annual precipitation is projected to increase by 1.8% to 11% under various RCP scenarios [43].

Additionally, the trends in predicted minimum and maximum temperatures were significantly positive under the RCP4.5 and RCP8.5 scenarios, at all the climate stations studied. Research conducted in different regions, such as Tehran in Iran [44], Yunnan province in China [38], and Sohra in India [45], consistently predicted rises in temperature under the RCP4.5 and RCP8.5 scenarios. These studies demonstrate the ability of SDSM to downscale climate variables and highlight the consistency of warming trends predicted under various RCP scenarios in different geographical locations.

It is important to point out that the largest increases in forecasted temperatures were recorded particularly in the months of June, September, October, and November. This suggests that the summer season may intensify earlier and that the annual warm period might extend beyond the traditional summer months. These results are in line with those performed by [46,47].

Overall, the present study is highly relevant for obtaining an accurate understanding of future climatic and meteorological trends in both the Ziz and Guir watersheds, which are characterized by an arid climate. The integration of ERA5 reanalysis data with observed station data allowed us to evaluate the performance of ERA5 in Morocco's arid climate and improve the temporal and geographical coverage of climate data, particularly in regions where observation stations are sparse or absent. However, it is important to acknowledge that the use of reanalysis data may introduce uncertainties related to the resolution and accuracy of the dataset, especially in complex terrains or areas with limited observational records.

Forecasting precipitation and minimum and maximum temperatures in arid regions is crucial due to the vulnerability of these areas to extreme weather conditions. It contributes to water and food security, helps anticipate extreme weather events, and promotes adaptation to climate change. The SDSM primarily works with General Circulation Models (GCMs) to generate downscaled climate projections. However, this presents a limitation, as SDSM does not directly support other types of climate models, such as Regional Climate Models (RCMs) or Earth System Models (ESMs). Employing a multi-model ensemble approach could help capture a broader range of possible outcomes and enhance the robustness of downscaled projections by reducing model-specific biases and uncertainties.

Despite these limitations, the findings of this study provide valuable insights into local climate trends and demonstrate the practical utility of statistical downscaling in regional climate assessments. These projections can serve as an important tool for decision-making in water resource management, agriculture, and disaster preparedness, enabling arid communities to better prepare for the environmental and climatic challenges they face.

5. Conclusions

The Statistical Downscaling Model (SDSM) was applied under the RCP4.5 and RCP8.5 scenarios to downscale precipitation and temperature values for the Ziz and Guir watersheds using station data and ERA5 reanalysis. The results indicate that ERA5 can serve as a valid alternative to station observations in these arid regions.

After calibration and validation, the SDSM model demonstrated good performance in simulating daily precipitation and temperatures (minimum and maximum). The trend analysis of the forecasted temperatures revealed a significant increase in both minimum and maximum temperatures under both scenarios, with increases reaching 1.84 °C and 2.39 °C by the end of the century for minimum temperatures under the RCP4.5 and RCP8.5 scenarios, respectively. For maximum temperatures, the RCP4.5 and RCP8.5 scenarios predict an increase of 1.78 °C and 2.9 °C, respectively. The highest increases are forecast for

June, September, October, and November, suggesting an extension of the warm period into traditionally cooler months. Precipitation forecasts showed a significant negative trend under the RCP4.5 scenario at the Ait Haddou station. Under RCP8.5, a negative trend is observed at the Sidi Hamza, Ait Haddou, Tit N'Aissa, and Bouanane stations, with a positive trend at the Hassan Addakhil dam station.

These projections indicate that the climate in the studied arid regions is becoming drier due to rising temperatures, necessitating specific adaptation strategies to mitigate the impacts of climate change. Therefore, we recommend the following measures: (i) Water resource management: Prioritize efficient water use through water-saving technologies, sustainable irrigation systems, and rainwater harvesting techniques to ensure water availability during drought periods; (ii) Agricultural practices: Enhance crop resilience by introducing drought-tolerant crops, adjusting planting schedules, and adopting soil conservation techniques to reduce the risk of crop failure and preserve soil moisture; (iii) Disaster preparedness: Establish early warning systems and community-based risk management plans to help vulnerable communities anticipate extreme weather events and take proactive measures to reduce their impacts.

Author Contributions: Conceptualization, S.D.; methodology, A.L. and H.T.; software, S.D.; validation, S.D. and L.B.; formal analysis, A.L. and H.T.; investigation, S.D.; resources, S.D.; data curation, S.D.; writing—original draft preparation, H.T.; writing—review and editing, L.B.; visualization, S.D. and L.B.; supervision, L.B.; project administration, A.L.; funding acquisition, A.L. All authors have read and agreed to the published version of the manuscript.

Funding: This research received no external funding.

Data Availability Statement: The data shared in this paper are in accordance with consent provided by participants on the use of confidential data. The Authors of this paper ensure that the publication of such data does not compromise the anonymity of the participants or breach local data protection laws.

Acknowledgments: The climatic and hydrometric data used in this study are available on request from the Hydraulic Basin Agency of Guir-Ziz-Rheris. This research is carried out with the assistance of the Hassan II Academy of Sciences and Technology, Rabat (Morocco).

Conflicts of Interest: The authors declare no conflicts of interest.

References

1. Adjei, V.; Amaning, E.F. Low Adaptive Capacity in Africa and Climate Change Crises. *J. Atmos. Sci. Res.* **2021**, *4*, 1–10. [[CrossRef](#)]
2. IPCC. *Mitigation of Climate Change: The Working Group III Contribution to the IPCC 4th Assessment Report*; IPCC: Geneva, Switzerland, 2009.
3. Orłowsky, B.; Seneviratne, S.I. Global Changes in Extreme Events: Regional and Seasonal Dimension. *Clim. Chang.* **2012**, *110*, 669–696. [[CrossRef](#)]
4. Almazroui, M.; Saeed, F.; Saeed, S.; Islam, M.N.; Ismail, M.; Klutse, N.A.B.; Siddiqui, M.H. Projected Change in Temperature and Precipitation Over Africa from CMIP6. *Earth Syst. Environ.* **2020**, *4*, 455–475. [[CrossRef](#)]
5. Waha, K.; Krümmenauer, L.; Adams, S.; Aich, V.; Baarsch, F.; Coumou, D.; Fader, M.; Hoff, H.; Jobbins, G.; Marcus, R.; et al. Climate Change Impacts in the Middle East and Northern Africa (MENA) Region and Their Implications for Vulnerable Population Groups. *Reg. Environ. Chang.* **2017**, *17*, 1623–1638. [[CrossRef](#)]
6. Ghosh, S.; Misra, C. Assessing Hydrological Impacts of Climate Change: Modeling Techniques and Challenges. *TOHYD* **2010**, *4*, 115–121. [[CrossRef](#)]
7. Marengo, J.; Ambrizzi, T. Use of Regional Climate Models in Impacts Assessments and Adaptations Studies from Continental to Regional and Local Scales: The CREAS (Regional Climate Change Scenarios for South America) Initiative in South America. In *Proceedings of the 8th ICSHMO, Foz do Iguagu, Brazil, 24–28 April 2006*; pp. 291–296.
8. Zittis, G.; Hadjinicolaou, P.; Klangidou, M.; Proestos, Y.; Lelieveld, J. A Multi-Model, Multi-Scenario, and Multi-Domain Analysis of Regional Climate Projections for the Mediterranean. *Reg. Environ. Chang.* **2019**, *19*, 2621–2635. [[CrossRef](#)]
9. Simonneaux, V.; Cheggour, A.; Deschamps, C.; Mouillot, F.; Cerdan, O.; Le Bissonnais, Y. Land Use and Climate Change Effects on Soil Erosion in a Semi-Arid Mountainous Watershed (High Atlas, Morocco). *J. Arid. Environ.* **2015**, *122*, 64–75. [[CrossRef](#)]

10. Hammoudy, W.; Ilmen, R.; Sinan, M. Climate Change and Its Impacts in Extreme Events in Morocco (Observation, Monitoring, and Forecasting). *J. Water Clim. Chang.* **2024**, *15*, 5817–5842. [[CrossRef](#)]
11. Moutia, S.; Sinan, M. Drought Projection from CMIP6 Climate Models over Morocco in the 21st Century Using the Standardized Precipitation Evapotranspiration Index (SPEI). In Proceedings of the E3S Web of Conferences, Laayoune, Morocco, 9 February 2024; Volume 489, p. 04003. [[CrossRef](#)]
12. Huebener, H.; Kerschgens, M. Downscaling of current and future rainfall climatologies for southern Morocco. Part I: Downscaling method and current climatology. *Int. J. Clim.* **2007**, *27*, 1763–1774. [[CrossRef](#)]
13. Born, K.; Christoph, M.; Fink, A.H.; Knippertz, P.; Paeth, H.; Speth, P. Moroccan Climate in the Present and Future: Combined View from Observational Data and Regional Climate Scenarios. In *Climatic Changes and Water Resources in the Middle East and North Africa*; Zereini, F., Hötzl, H., Eds.; Environmental Science and Engineering; Springer: Berlin/Heidelberg, Germany, 2008; pp. 29–45, ISBN 978-3-540-85046-5.
14. Born, K.; Fink, A.H.; Paeth, H. Dry and Wet Periods in the Northwestern Maghreb for Present Day and Future Climate Conditions. *Meteorol. Z.* **2008**, *17*, 533–551. [[CrossRef](#)]
15. Driouech, F.; Déqué, M.; Sánchez-Gómez, E. Weather Regimes—Moroccan Precipitation Link in a Regional Climate Change Simulation. *Glob. Planet. Chang.* **2010**, *72*, 1–10. [[CrossRef](#)]
16. Hersbach, H.; Bell, B.; Berrisford, P.; Hirahara, S.; Horányi, A.; Muñoz-Sabater, J.; Nicolas, J.; Peubey, C.; Radu, R.; Schepers, D.; et al. The ERA5 Global Reanalysis. *Q. J. R. Meteorol. Soc.* **2020**, *146*, 1999–2049. [[CrossRef](#)]
17. Wilby, R.L.; Dawson, C.W.; Barrow, E.M. Sdsm—A Decision Support Tool for the Assessment of Regional Climate Change Impacts. *Environ. Model. Softw.* **2002**, *17*, 145–157. [[CrossRef](#)]
18. Tang, J.; Niu, X.; Wang, S.; Gao, H.; Wang, X.; Wu, J. Statistical Downscaling and Dynamical Downscaling of Regional Climate in China: Present Climate Evaluations and Future Climate Projections. *JGR Atmos.* **2016**, *121*, 2110–2129. [[CrossRef](#)]
19. Le Roux, R.; Katurji, M.; Zawar-Reza, P.; Quénol, H.; Sturman, A. Comparison of Statistical and Dynamical Downscaling Results from the WRF Model. *Environ. Model. Softw.* **2018**, *100*, 67–73. [[CrossRef](#)]
20. Attique, R.; Rientjes, T.; Booi, M. Comparison between Statistical and Dynamical Downscaling of Rainfall over the Gwadar-Ormara Basin, Pakistan. *Meteorol. Appl.* **2023**, *30*, e2151. [[CrossRef](#)]
21. Cheng, Y.; Chen, H.; Xu, C. Comparison of Dynamical and Statistical Downscaling in Climate Change Impact Study in Hanjiang Basin. In Proceedings of the 35th IAHR World Congress, Chengdu, China, 8–13 September 2013.
22. Haq, M.A.; Ahmed, A.; Gyani, J. Intercomparison of Machine Learning and Statistical Downscaling for Climatic Parameters: A Case Study of Bhuntar, Himachal Pradesh. *ADAS* **2024**, *92*, 191–209. [[CrossRef](#)]
23. Sami, S.S.; Ali, A.A.; Jalal, A.D. An Application of the Statistical Downscaling Model (SDSM) to Simulate Precipitation Data in the Iraqi Western Desert. In Proceedings of the 2nd International Conference for Engineering Sciences and Information Technology (ESIT 2022): ESIT2022 Conference Proceedings, Al Anbar, Iraq, 17–18 August 2024; p. 030113.
24. Chim, K.; Tunncliffe, J.; Shamseldin, A.; Chan, K. Identifying Future Climate Change and Drought Detection Using CanESM2 in the Upper Siem Reap River, Cambodia. *Dyn. Atmos. Ocean.* **2021**, *94*, 101182. [[CrossRef](#)]
25. Javaherian, M.; Ebrahimi, H.; Aminnejad, B. Prediction of Changes in Climatic Parameters Using CanESM2 Model Based on Rcp Scenarios (Case Study): Lar Dam Basin. *Ain Shams Eng. J.* **2021**, *12*, 445–454. [[CrossRef](#)]
26. Seng, C.K.; Weng, T.K.; Nakayama, A. Development of Statistically Downscaled Regional Climate Model Based on Representative Concentration Pathways for Ipoh, Subang and KLIA Sepang in Peninsular Malaysia. *IOP Conf. Ser. Earth Environ. Sci.* **2021**, *945*, 012022. [[CrossRef](#)]
27. Gebrechorkos, S.H.; Hülsmann, S.; Bernhofer, C. Statistically Downscaled Climate Dataset for East Africa. *Sci. Data* **2019**, *6*, 31. [[CrossRef](#)]
28. Jones, C.; Robertson, E.; Arora, V.; Friedlingstein, P.; Shevliakova, E.; Bopp, L.; Brovkin, V.; Hajima, T.; Kato, E.; Kawamiya, M.; et al. Twenty-First-Century Compatible CO₂ Emissions and Airborne Fraction Simulated by CMIP5 Earth System Models under Four Representative Concentration Pathways. *J. Clim.* **2013**, *26*, 4398–4413. [[CrossRef](#)]
29. Arora, V.K.; Scinocca, J.F.; Boer, G.J.; Christian, J.R.; Denman, K.L.; Flato, G.M.; Kharin, V.V.; Lee, W.G.; Merryfield, W.J. Carbon Emission Limits Required to Satisfy Future Representative Concentration Pathways of Greenhouse Gases: Allowable Future Carbon Emissions. *Geophys. Res. Lett.* **2011**, *38*, L05805.1–L05805.6. [[CrossRef](#)]
30. Tachiiri, K.; Hargreaves, J.C.; Annan, J.D.; Huntingford, C.; Kawamiya, M. Allowable Carbon Emissions for Medium-to-High Mitigation Scenarios. *Tellus B Chem. Phys. Meteorol.* **2013**, *65*, 20586. [[CrossRef](#)]
31. Kendall, M.G. *Rank Correlation Methods*; Charles Griffin: London, UK, 1975; p. 160.
32. Mann, H.B. Nonparametric Tests against Trend. *Econometrica* **1945**, *13*, 245–259. [[CrossRef](#)]
33. Sen, P.K. Estimates of the Regression Coefficient Based on Kendall’s Tau. *J. Am. Stat. Assoc.* **1968**, *63*, 1379–1389. [[CrossRef](#)]
34. Draper, N.R.; Smith, H. *Applied Regression Analysis*, 3rd ed.; Wiley Series in Probability and Statistics; Wiley: New York, NY, USA, 1998; ISBN 978-0-471-17082-2.

35. Kim, M.; Lee, E. Validation and Comparison of Climate Reanalysis Data in the East Asian Monsoon Region. *Atmosphere* **2022**, *13*, 1589. [[CrossRef](#)]
36. Sheridan, S.C.; Lee, C.C.; Smith, E.T. A Comparison Between Station Observations and Reanalysis Data in the Identification of Extreme Temperature Events. *Geophys. Res. Lett.* **2020**, *47*, GL088120. [[CrossRef](#)]
37. Wilby, R.L.; Dawson, C.W. The Statistical DownScaling Model: Insights from One Decade of Application. *Int. J. Clim.* **2013**, *33*, 1707–1719. [[CrossRef](#)]
38. Liu, J.; Chen, S.; Li, L.; Li, J. Statistical Downscaling and Projection of Future Air Temperature Changes in Yunnan Province, China. *Adv. Meteorol.* **2017**, *2017*, 2175904. [[CrossRef](#)]
39. Suo, M.Q.; Zhang, J.; Zhou, Q.; Li, Y.P. Applicability Analysis of SDSM Technology to Climate Simulation in Xingtai City, China. *IOP Conf. Ser. Earth Environ. Sci.* **2019**, *223*, 012053. [[CrossRef](#)]
40. Rahman, G.; Rahman, A.; Munawar, S.; Moazzam, M.F.U.; Dawood, M.; Miandad, M.; Panezai, S. Trend Analysis of Historical and Future Precipitation Projections over a Diverse Topographic Region of Khyber Pakhtunkhwa Using SDSM. *J. Water Clim. Chang.* **2022**, *13*, 3792–3811. [[CrossRef](#)]
41. El Hafyani, M.; Essahlaoui, N.; Essahlaoui, A.; Mohajane, M.; Van Rompaey, A. Generation of Climate Change Scenarios for Rainfall and Temperature Using SDSM in a Mediterranean Environment: A Case Study of Boufakrane River Watershed, Morocco. *J. Umm Al-Qura Univ. Appl. Sci.* **2023**, *9*, 436–448. [[CrossRef](#)]
42. El-Yazidi, M.; Benabdelhadi, M.; Laaraj, M.; Boutallaka, M.; El-Hamdouny, M.; Daide, F.; Tabyaoui, H.; Lahrach, A. Comparative Study of Observed and Projected Future Climate Evolution in Two Watersheds (Souss-Massa and Ouergha, Morocco) Using the Statistical Downscaling Model (SDSM). In Proceedings of the BIO Web of Conferences, Fez, Morocco, 25 June 2024; Volume 115, p. 03003. [[CrossRef](#)]
43. Shivam, G.; Goyal, M.K.; Sarma, A.K. Index-Based Study of Future Precipitation Changes over Subansiri River Catchment under Changing Climate. *J. Environ. Inform.* **2017**, *34*, 1–14. [[CrossRef](#)]
44. Shakeri, H.; Motiee, H.; McBean, E. Projection of Important Climate Variables in Large Cities under the CMIP5–RCP Scenarios Using SDSM and Fuzzy Downscaling Models. *J. Water Clim. Chang.* **2021**, *12*, 1802–1823. [[CrossRef](#)]
45. Kalita, R.; Kalita, D.; Saxena, A. Future Projections of Precipitation and Temperature Extremes at Sohra (Cherrapunji) Using Statistical Downscaling Model. *MAUSAM* **2024**, *75*, 181–190. [[CrossRef](#)]
46. Ho, C.-H.; Park, C.-K.; Yun, J.; Lee, E.-J.; Kim, J.; Yoo, H.-D. Asymmetric Expansion of Summer Season on May and September in Korea. *Asia-Pac. J. Atmos. Sci.* **2020**, *57*, 619–627. [[CrossRef](#)]
47. Park, B.-J.; Min, S.-K.; Weller, E. Lengthening of Summer Season over the Northern Hemisphere under 1.5 °C and 2.0 °C Global Warming. *Environ. Res. Lett.* **2021**, *17*, 014012. [[CrossRef](#)]

Disclaimer/Publisher’s Note: The statements, opinions and data contained in all publications are solely those of the individual author(s) and contributor(s) and not of MDPI and/or the editor(s). MDPI and/or the editor(s) disclaim responsibility for any injury to people or property resulting from any ideas, methods, instructions or products referred to in the content.